JACS
JOURNAL OF THE AMERICAN CHEMICAL SOCIETY
Article
pubs.acs.org/JACS

Homogeneous Catalysis Under Ultradilute Conditions: TAML/NaClO Oxidation of Persistent Metaldehyde

Liang L. Tang,[†] Matthew A. DeNardo,[†] Christopher J. Schuler,[†] Matthew R. Mills,[†] Chakicherla Gayathri,[†] Roberto R. Gil,[†] Rakesh Kanda,[‡] and Terrence J. Collins*[,†]

[†]Institute for Green Science, Department of Chemistry, Carnegie Mellon University, 4400 Fifth Avenue, Pittsburgh, Pennsylvania 15213, United States

[‡]Institute for the Environment, Brunel University, Halsbury Building (130), Kingston Lane, Uxbridge, Middlesex, UB8 3PH, United Kingdom

Supporting Information

ABSTRACT: TAML activators enable homogeneous oxidation catalysis where the catalyst and substrate (S) are ultradilute (pM–low μM) and the oxidant is very dilute (high nM–low mM). Water contamination by exceptionally persistent micropollutants (MPs), including metaldehyde (Met), provides an ideal space for determining the characteristics and utilitarian limits of this ultradilute catalysis. The low MP concentrations decrease throughout catalysis with S oxidation (k_{II}) and catalyst inactivation (k_i) competing for the active catalyst. The percentage of substrate converted (%Cvn) can be increased by discovering methods to increase k_{II}/k_i. Here we show that NaClO extends catalyst lifetime to increase the Met turnover number (TON) 3-fold compared with H_2O_2, highlighting the importance of oxidant choice as a design tool in TAML systems. Met oxidation studies (pH 7, D_2O, 0.01 M phosphate, 25 °C) monitored by ^{1}H NMR spectroscopy show benign acetic acid as the only significant product. Analysis of TAML/NaClO treated Met solutions employing successive identical catalyst doses revealed that the processes can be modeled by the recently published relationship between the initial and final [S] (S_0 and S_∞, respectively), the initial [catalyst] (Fe_{Tot}) and k_{II}/k_i. Consequently, this study establishes that ΔS is proportional to S_0 and that the %Cvn is conserved across all catalyst doses in multicatalyst-dose processes because the rate of the k_{II} process depends on [S] while that of the k_i process does not. A general tool for determining the Fe_{Tot} required to effect a desired %Cvn is presented. Examination of the dependence of TON on k_{II}/k_i and Fe_{Tot} at a fixed S_0 indicates that for any TAML process employing $Fe_{Tot} < 1 \times 10^{-6}$ M, small catalyst doses are not more efficient than one large dose.

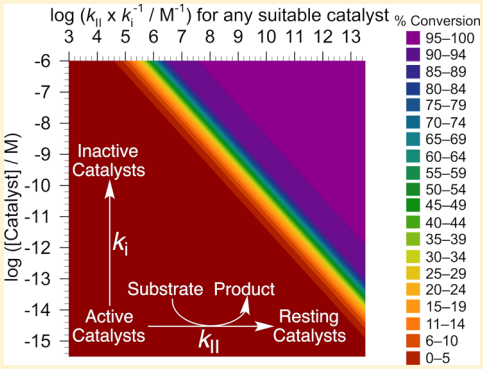

INTRODUCTION

The development of homogeneous oxidation catalysis that is effective under ultradilute conditions promises to enable a new branch of chemistry with implications for sustainability. For example, micropollutants (MPs) produce adverse effects in aquatic organisms at environmentally relevant low parts per billion (ppb) to low parts per trillion (ppt) concentrations.[1,2] Currently, Switzerland is installing end-of-plant ozone and activated carbon (AC) technologies for reducing MP concentrations in municipal wastewater, but both are expensive.[3] TAML catalyzed peroxide oxidations of MPs function so well under ultradilute conditions (low ppb, low nM) that novel and cheaper processes for the removal of MPs are now within reach.[4−12] TAML/H_2O_2 has been shown to remove low ppb–low ppt (low nM–low pM) concentrations of MPs of highest concern from London municipal wastewater with comparable technical performance to ozone and projected superior cost performance.[13] Certain MPs are not effectively removed from water by ozone or AC.[14] For example, metaldehyde (Met, Chart 1) is so persistent that very expensive advanced oxidation processes (e.g., UV/H_2O_2) need to be applied when drinking water is unacceptably contaminated.[15−17] A discussion of the challenges Met poses to water

Chart 1. Structures of the Metaldehyde I (M I) Diastereomer of Metaldehyde and TAML[a] Compounds 1

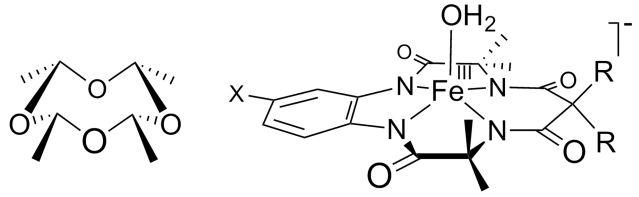

[a]TAML is a registered trademark covering tetra-amido-*N* macrocyclic ligand complexes.[18]

Received: October 25, 2016
Published: December 6, 2016

DOI: 10.1021/jacs.6b11145
J. Am. Chem. Soc. 2017, 139, 879–887

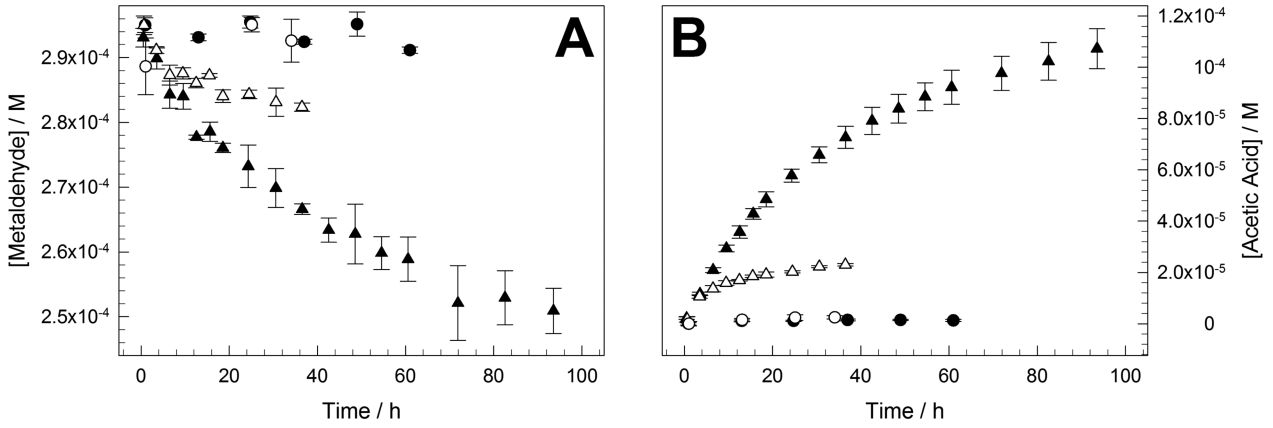

Figure 1. Oxidation of Met (2.95×10^{-4} M) by NaClO (3.8×10^{-3} M, 13 equiv) or H_2O_2 (3.61×10^{-3} M, 12 equiv) at pH 7. Kinetic traces of (A) metaldehyde consumption and (B) acetic acid formation. Circles: metaldehyde plus oxidant control experiments (● NaClO and ○ H_2O_2). Triangles: **1a** (3.98×10^{-7} M) catalyzed oxidations (▲ NaClO and △ H_2O_2). Conditions: pH 7 D_2O (0.01 M, phosphate), reactions were allowed to proceed at room temperature. Concentrations were calculated from the absolute integrals of the metaldehyde and acetic acid CH_3 signals at 1.34 and initially at 1.92 ppm, respectively. The initial ^{1}H NMR integrals for the trace amounts of acetic acid that formed on sonication of metaldehyde were subtracted from those of the total acetic acid.

treatment and available removal methods has been published,[14] and a more thorough list of the available Met removal methods can be found in the Supporting Information of this work (Tables S1−S3). Therefore, we have explored TAML catalysis of Met oxidation. Met oxidation exacts the most demanding performance of TAML/H_2O_2 systems studied to date.[14] We have shown that **1a**/H_2O_2 (Chart 1) is capable of oxidizing Met. However, in contrast with most MPs, both the **1a**/H_2O_2 rates of Met oxidation and the balance between these and the rates of catalyst inactivation were too unfavorable to promise a real-world solution. Therefore, we have identified Met as a boundary case, one for which effective oxidation will be either just possible or just not possible. By working to improve the technical performance in this extreme case, we have encountered a significant advantage resulting from changing the oxidant from H_2O_2 to hypochlorite. Hypochlorite is widely employed in US water disinfection processes[1] where it is generated in situ from chlorine gas at a low cost.[19] We have long known that TAML activators catalyze hypochlorite reactions.[20] NaClO activates TAML catalysts to give Fe^V=O complexes from −40 °C[21] to room temperature,[22] highlighting a similarity with the most reactive intermediates in TAML/H_2O_2 systems.[23]

Here we examine the **1a** (0.4−6.4 μM) catalyzed degradation of Met (0.33 mM) by NaClO (0.008−0.02 M) at 25 °C and pH 7 (0.01 M phosphate) in D_2O. The shift from **1a**/H_2O_2 to **1a**/NaClO results in a 3-fold improvement in process technical performance, establishing that oxidant choice is an important process design parameter for these systems. Effective oxidation of the very resistant Met required the addition of multiple catalyst doses over which a consistent relationship was found between $[Met]_0$ (initial [Met]) and the Δ[Met] which held for all 18 sequential catalyst treatments. These results have served as an entry point for augmenting the mathematical logic which models TAML catalysis and for developing a 3-D map that will typically allow prediction of the percent conversion (%Cvn) of any ultradilute concentration of a substrate by any TAML catalyst under broadly specified conditions. The map holds considerable promise as a tool for TAML-based water purification. It predicts the amount of catalyst needed to achieve a targeted substrate removal and identifies boundary pollutants that are exceptionally difficult to treat with the current set of TAML catalysts. Finally, we show that when [TAML] < 1×10^{-6} M, the efficiency of oxidation of easily oxidized pollutants is inversely related to [TAML] because the substrate undergoes dilution, while in the transformation of boundary pollutants TON is largely independent of [TAML].

MATERIALS AND METHODS

Materials. All reagents, components of buffered solutions, and solvents were of at least ACS reagent grade and were used as received. Met (Acros, 99%) was recrystallized in ethanol[24] and stored at 4 °C. Since three isomers of Met, each having a distinct infrared (IR) spectrum, are known, the IR spectrum of the recrystallized sample was recorded (Figure S1). The spectrum is nearly identical to that previously assigned[25] to the metaldehyde I (M I) diastereomer, the most abundant form of Met, the structure of which was previously determined by X-ray crystallography (Chart 1).[26] Met stock solutions (0.3 mM) were prepared by sonicating the appropriate amount of Met in buffered D_2O (99.9%, Cambridge Isotope Laboratories, Inc.) at room temperature for 3 h. Buffers of the desired pH's (6.2−7.0) were prepared with 0.01 M phosphate and monitored by an Accumet AB15 pH meter at room temperature. A solution of DCl in D_2O was added to adjust the reaction mixture pH to 7 after NaClO addition. The reported values are the uncorrected pH meter readings. TAML activator **1a** was provided by GreenOx Catalysts Inc. Stock solutions of **1a** (2×10^{-4} M) were prepared in D_2O and stored at 4 °C. H_2O_2 and NaClO solutions were standardized daily by measuring the absorbances at 230 nm (ε = 72.4 M^{-1} cm^{-1})[27] and 293 nm (ε = 350 M^{-1} cm^{-1}),[28] respectively. The specified [NaClO] values are those of the added reagent; at pH 7 NaClO is ca. 70% HOCl.

Instrumental. IR measurements were performed on a Mattson ATI Affinity 60 AR FTIR spectrometer using KBr pellets. UV−vis measurements were performed on an Agilent 8453 UV−vis spectrophotometer equipped with an 8-cell transporter and thermostatic temperature controller. Solution temperatures were maintained at 25 °C in capped quartz cuvettes (1.0 cm).

TAML catalysis of metaldehyde oxidation was followed by ^{1}H NMR. 1D ^{1}H spectra were recorded at 300 K on a Bruker Avance III 500 NMR spectrometer operating at 500.13 MHz. The water signal was suppressed using the presaturation experiment (zgpr) from the Bruker pulse programs library. Chemical shifts are reported in parts per million relative to TMSP (an internal standard for aqueous solutions). However, since TAML catalyzed oxidation of an internal standard could interfere with measurements, none was added.[14] Each sample was scanned 128 times over 16.5 min. The Bruker TopSpin 3.0

DOI: 10.1021/jacs.6b11145
J. Am. Chem. Soc. 2017, 139, 879−887

Table 1. Comparison of 1a/NaClO and 1a/H_2O_2 Systems in Catalysis of Metaldehyde Degradation at pH 7[a]

oxidant	$v \times 10^8$/M min^{-1}[b]	removal/%	major products	TON	functioning time
NaClO	2.4 ± 0.4	14.4 ± 0.9	acetic acid	106 ± 6	80 h
H_2O_2	2.2 ± 0.3	4.3 ± 0.7	acetaldehyde and acetic acid	32 ± 5	10 h

[a]Conditions: [Met] = 2.95×10^{-4} M, [**1a**] = 3.98×10^{-7} M, [NaClO] = 3.8×10^{-3} M, [H_2O_2] = 3.6×10^{-3} M. [b]The rate (v) is calculated from the slope of the line of best fit to the first three [Met] measurements (v = d[Met]/dt).

software was used to process the NMR data. The Met $(C\underline{H}_3CHO)_4$ and acetic acid $C\underline{H}_3COOH$ absolute integrals were used for quantification. Each data point is the average of three measurements, and the associated error is the standard deviation of the set.

RESULTS AND DISCUSSION

The choice of oxidant is a process design tool for advancing TAML catalyst lifetimes. To assess the relative performances of **1a**/NaClO and **1a**/H_2O_2, ^{1}H NMR measurements were performed on Met solutions in D_2O under identical conditions. As shown in Figure 1A, the [Met] is unaffected by either NaClO or H_2O_2 alone. The NaClO kinetic trace shows that a single **1a** dose giving a [**1a**] of 3.98×10^{-7} M effects a 14.4% conversion (14.4%Cvn) as indicated by a reduction in the absolute integral of the 1.34 ppm Met $C\underline{H}_3$ signal over the approximate duration of catalysis of 80 h (Table 1). For comparison, in the corresponding **1a**/H_2O_2 experiment, a 4.3% Cvn is observed over the approximate duration of catalysis, which this time lasted only 10 h. In both cases, the relationship between [Met] and time is initially linear allowing calculation of the initial oxidation rates (v = d[S]/dt) by fitting a linear form. While the initial rates of Met consumption are identical, a turnover number (TON) of 106 is observed in the NaClO system compared with 32 in the H_2O_2 system, a 3-fold improvement. These reaction features are also visible in the kinetic traces for acetic acid production (Figure 1B), with ca. 5 times more acetic acid being produced by **1a**/NaClO. Under these conditions **1a**/H_2O_2 generates an acetic acid/acetaldehyde product ratio of 3:1. The respective acetic acid and acetaldehyde rat LD_{50} values are 3310 and 661 mg kg^{-1} suggesting that selectivity for acetic acid is desirable.[29] The near-exclusive production of acetic acid by **1a**/NaClO leads to an even more benign product mixture. Because chlorination of water containing organic matter generates hazardous disinfection byproducts (DBPs), including carcinogenic chloroform,[30,31] we have monitored for chloroform production; none was detected within the limits of the NMR technique.

The identical initial rates of Met oxidation observed for NaClO and H_2O_2 are informative. TAML catalysts function via the stoichiometric mechanism of Scheme 1. The resting catalysts (Fe^{III}) undergo activation by an oxidant (Ox, k_I) to form active catalysts (Ac) which then oxidize a substrate (S) to give Fe^{III} and product(s) (k_{II}) or undergo inactivation (k_i or k_{2i})—the reverse of catalyst activation, k_{-I}, is kinetically negligible.

Scheme 1. General Mechanism of TAML Catalysis

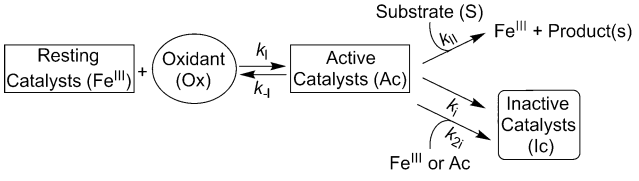

Equation 1 models the initial rate of substrate oxidation (Fe_{Tot} is the total concentration of catalyst).[35] For particularly difficult to oxidize substrates, catalyst activation outpaces substrate oxidation (k_I[Ox] > k_{II}[S]) and eq 1 simplifies to eq 2.

$$v = \frac{k_I k_{II}[\mathrm{Ox}][\mathrm{S}]}{k_{-I} + k_I[\mathrm{Ox}] + k_{II}[\mathrm{S}]}\mathrm{Fe_{Tot}} \quad (1)$$

$$v = k_{II}[\mathrm{S}]\mathrm{Fe_{Tot}} \quad (2)$$

Substrate oxidation and catalyst inactivation compete for Ac. Recently, we have developed eq 3,[32] a mathematical form that models the final result of this competition, S_∞ (S_0 and S_∞ are the initial and final [S], respectively). Equation 3 applies only when there is an excess of the primary oxidant and substrate consumption is incomplete ($S_\infty > 0$), i.e. conditions are set such that the catalyst is the limiting species and is completely inactivated before all of the substrate has been oxidized. These conditions were employed in the Met oxidation experiments described herein.

$$\ln \frac{S_0}{S_\infty} = \frac{k_{II}}{k_i}\mathrm{Fe_{Tot}} \quad (3)$$

For most TAML processes, k_I[Ox] < k_{II}[S] and catalyst activation is rate determining. However, Met oxidation by Ac is extremely slow. Of the tested TAML/H_2O_2 processes,[14] the **1a** system is known to deliver the highest measurable v and %Cvn. The eq 3 estimated k_{II} value for **1a**/H_2O_2 is 120 ± 30 M^{-1} s^{-1}, ca. 340 times lower than the corresponding value for Orange II of 41 000 ± 1000 M^{-1} s^{-1}, noting of course that the Orange II k_{II} and k_i were measured in H_2O while the Met data were recorded in D_2O.[33] Given this value, the **1a**/H_2O_2 (D_2O) Met process exhibits the lowest k_{II} (and %Cvn, see later) at pH 7 of any MP oxidation studied to date. The eq 3 estimated **1a**/H_2O_2 (D_2O) Met k_{II} is comparable to the **1a**/H_2O_2 (D_2O) k_I of 180 ± 8 M^{-1} s^{-1}. Since $k_I \sim k_{II}$ for this Met system, and [H_2O_2] > 10 × [Met], the oxidation of this very difficult substrate by Ac is rate-determining and eq 2 applies. This is further supported by the similarity of the rates for both oxidants which also provides strong evidence for rate determining substrate oxidation by a common Ac. Noting again that acetaldehyde is observed in the **1a**/H_2O_2 (D_2O) study, it follows that the known oxidation of acetaldehyde by NaClO[34] probably accounts for the virtual absence of acetaldehyde in the **1a**/NaClO product mixture. Since, as indicated by eq 3, ln S_0/S_∞ is fixed by $k_{II}Fe^{III}{}_{Tot}/k_i$, and both the NaClO and H_2O_2 processes share a common rate-determining step with a common Ac, the NaClO performance advantage must derive from a decrease in k_i which is reflected in the greater reduction in [Met] and longer operating time. The **1a**/NaClO k_i value matches that of **1b**/H_2O_2.[33] Since the **1a** Ac oxidizes substrates ca. 1 order of magnitude faster than **1b**, this amounts to a k_{II}/k_i gain of ca. 1 order of magnitude on going from the **1b**/H_2O_2 to **1a**/NaClO systems. Considering that k_{II} and k_i have been found to track linearly for all TAML catalysts,

DOI: 10.1021/jacs.6b11145
J. Am. Chem. Soc. 2017, 139, 879–887

this gain in operational stability with preservation of oxidative activity is remarkable.[33]

The inactivation of TAML catalysts has been found to follow both intramolecular suicidal[35−37] and intermolecular H_2O_2-dependent pathways[36,38] which are unimolecular in catalyst. To minimize the performance reducing impacts of the latter in ultradilute catalysis, a low $[H_2O_2]$ is generally employed. In one case, a system in which H_2O_2 is generated enzymatically in situ has been devised.[39] By using NaClO, we have eliminated the H_2O_2-dependent catalyst inactivation pathways altogether. The TON increases by 70% on changing from H_2O_2 to NaClO. The recently published **1a**/H_2O_2 k_i[33] of $(1.1 \pm 0.3) \times 10^{-3}$ s^{-1} is ca. 70% greater than the eq 3 estimated NaClO k_i value of $(3.0 \pm 0.8) \times 10^{-4}$ s^{-1}. These comparisons indicate that in D_2O, at least 70% of the k_i processes are attributable to H_2O_2 dependent catalyst inactivation. The lifetime extension observed for the **1a**/NaClO catalysis further establishes the importance of understanding the nature of the H_2O_2 dependent inactivation pathway in TAML/H_2O_2 catalysis.

Effects of Different Catalyst Concentrations. The identical initial rates of **1a**/H_2O_2 and **1a**/NaClO Met consumption are slow (Table 1). The effect of [**1a**] on the oxidation was examined with the aim of increasing both v and the %Cvn. Since the H_2O_2 %Cvn with [**1a**] = 3.98×10^{-7} M was small, only higher [**1a**] experiments were performed in the H_2O_2 system (Figure 1). Surprisingly, the increases in v and % Cvn anticipated on increasing the [**1a**] to 1.66×10^{-6} M were not observed. Instead, the kinetic trace is largely indistinguishable from that of the control experiment (Figures 2 and S5).

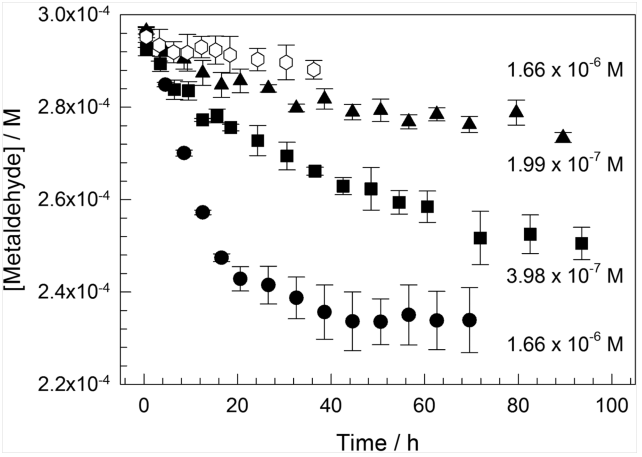

Figure 2. Kinetic traces of **1a** catalyzed metaldehyde oxidation. [**1a**] values are shown on the figure next to the corresponding kinetic traces. Hollow hexagons: $[H_2O_2] = 3.61 \times 10^{-3}$ M (12.2 equiv). Black symbols: $[NaClO] = 3.8 \times 10^{-3}$ M (12.8 equiv). Other conditions: pH 7 D_2O (0.01 M, phosphate), $[Met]_0 = 2.95 \times 10^{-4}$ M.

Kinetic traces of the oxidation of Met (2.95×10^{-4} M) by NaClO (3.8×10^{-3} M) were recorded for three different [**1a**] values: 1.99×10^{-7} M, 3.98×10^{-7} M, and 1.66×10^{-6} M (Figure 2). As shown in Table 2 and Figure S2, the initial rates of Met consumption increased linearly with [**1a**] but the TON did not remain constant. At [**1a**] of 1.99×10^{-7} M and 3.98×10^{-7} M, TONs of ∼100 are observed. However, at [**1a**] of 1.66×10^{-6} M, the TON decreased by ∼60%—the corresponding %Cvn values are 7.8, 14.4 and 21%. In each case, approximately half of the theoretical amount of acetic acid, the only observable major product, is produced (kinetic traces of acetic acid generation are shown in Figure S3). At the lower two [**1a**] values the NaClO catalysis is observed to function for about 90 h, but at the highest [**1a**] the catalysis lasts only 30 h. Typically, TAML catalysis is conducted with excess oxidant and stops when all of the catalyst is inactivated. Catalysis resumes upon introduction of a fresh TAML dose.[14,32,33,36] In the **1a**/NaClO experiment with $[\mathbf{1a}] = 1.66 \times 10^{-6}$ M, Met consumption did not resume after introducing an additional dose of **1a** or of NaClO (3.51×10^{-4} M) at 50 h (Figure S4), giving evidence for both irreversible catalyst inactivation and complete oxidant consumption. This behavior is unusual and is being examined further.

In both the H_2O_2 and NaClO systems, catalyst lifetime and TON diminished significantly on increasing [**1a**] from 1.99–3.98×10^{-7} M to 1.66×10^{-6} M. This suggested that higher order catalyst degradation processes in [**1a**] became kinetically relevant. We have previously considered the role of inactivation pathways that are bimolecular in catalyst, labeled k_{2i} processes (Scheme 1), in TAML catalysis, and estimated that contributions from such pathways are negligible at catalyst concentrations $<1 \times 10^{-6}$ M.[32,33,36,37] These experimental results support the prior estimates. The detection of these higher order processes here suggests a k_{2i} pathway in both systems. However, increasing [**1a**] impacted the H_2O_2 and NaClO processes differently. In the NaClO system, increasing [**1a**] from 3.98×10^{-7} M to 1.66×10^{-6} M gave a 6.6% increase in the percent of Met oxidized (Table 1). In the H_2O_2 system, this same [**1a**] increase reduced Met oxidation from 4.3% to effectively zero within experimental error (Figures 2 and S5). We have interpreted this loss of catalysis in the following way.

If for the H_2O_2 case with $[\mathbf{1a}] = 1.66 \times 10^{-6}$ M, eq 3 is applied using the estimated k_{II} of 120 ± 30 M^{-1} s^{-1} and setting an approximation for the oxidation percentage of 2% (Figure S5; to avoid a zero denominator), the estimated total k_i value is ca. 1.0×10^{-2} s^{-1}. This is an order of magnitude greater than the k_i for **1a**/H_2O_2 measured at [**1a**] ≈ 10^{-8} M where inactivation is exclusively unimolecular in catalyst.[33] These results suggest the operation of inactivation processes that are bimolecular in catalyst at [**1a**] ≥ ca. 1×10^{-6} M which greatly outpace those that are unimolecular in catalyst. Equation 3 is

Table 2. Summary of Metaldehyde Degradation at Different [1a] Values[a]

[**1a**] × 10^{-7} M	$v \times 10^8$/M min^{-1}[b]	TON	%Cvn	acetic acid formed/%[c]	t_∞[d]/h
1.99	1.2 ± 0.2	116 ± 6	7.8 ± 0.4	4.1 ± 0.1	90
3.98	2.0 ± 0.2	106 ± 6	14.4 ± 0.9	9.0 ± 0.7	90
16.6	5.4 ± 0.1	37 ± 5	21 ± 3	10 ± 1	30

[a]Conditions: [Met] = 2.95×10^{-4} M, [NaClO] ≈ 3.8×10^{-3} M. [b]The rate v was calculated from the slope of the line of best fit to the first five [Met] measurements (v = d[Met]/dt). [c]The percentage of acetic acid (AA) formation was calculated from the $C\underline{H}_3$ absolute integral relative to the initial metaldehyde signal ($(^{Abs}Int_{1.34})_0$, AA% = $(^{Abs}Int_{1.92})/(^{Abs}Int_{1.34})_0 \times 100$). [d]Reaction time.

DOI: 10.1021/jacs.6b11145
J. Am. Chem. Soc. 2017, 139, 879–887

very sensitive to the estimated oxidation percentage. If values <2% are chosen instead, even higher k_i values result. Application of eq 3 to the analogous NaClO process with [**1a**] = 1.66×10^{-6} M gives a k_i of 8.5×10^{-4} s^{-1}. This is at least 1 order of magnitude less than the corresponding H_2O_2 value and is comparable to the k_i value observed for the lower [**1a**] H_2O_2 systems. Thus, one can deduce that at high [**1a**], the use of NaClO results in productive catalysis by avoiding k_{2i} processes observed in the H_2O_2 system. However, the eq 3 calculated k_i for the [**1a**] = 1.66×10^{-6} M NaClO system is ca. 3-fold greater than that of the lower [**1a**] NaClO experiments, indicating that k_{2i} processes operate in the NaClO system. These results highlight the importance of developing kinetic approaches for determining the mechanism(s) and rate constant(s) of the k_{2i} process(es). Such studies are ongoing, and the understanding gained through them is expected to aide in the design of superior catalysts for high [TAML] processes.

More Complete Metaldehyde Removal with Continuous Additions of Catalyst and Oxidant. As a result of k_{2i} processes, deeper Met removals are more efficiently accomplished by using multiple catalyst doses to ensure that [**1a**] < ca. 1×10^{-6} M. The optimized catalyst dose was that giving a [**1a**] of 4×10^{-7} M. The data shown in Figure 3 represent two separate experiments demonstrating the efficacy of multiple catalyst doses each giving a [**1a**] of 4×10^{-7} M. Experiment 1 employed a $[Met]_0$ of 3.32×10^{-4} M (Figure 3 solid circles and Figure S6). Since Met mineralization requires 20 equiv of NaClO, a slight excess (7.61×10^{-3} M) was added. The first catalyst dose consumed Met for 72 h before the reaction ceased. Seven additional **1a** doses were added leading to a slow oxidation of 75.3% of the initial Met over 576 h. After the addition of the fifth catalyst dose, the position of the CH_3COO^{-1} ^1H NMR signal at 1.956 ppm indicated a solution pH of 5.2, 1.8 units less than the initial pH of 7 (Figure S7).[14,40] Therefore, at 360 h, enough additional NaClO was added to raise the [NaClO] by 4.79×10^{-3} M. This addition returned the CH_3COO^- signal to its initial value while providing additional oxidant. The initial metaldehyde concentration ($[Met]_0$), change in metaldehyde concentration (Δ[Met]), TON, and %Cvn for each catalyst dose are summarized in Table S4. For all catalyst doses, Δ[Met] and TON declined with $[Met]_0$.

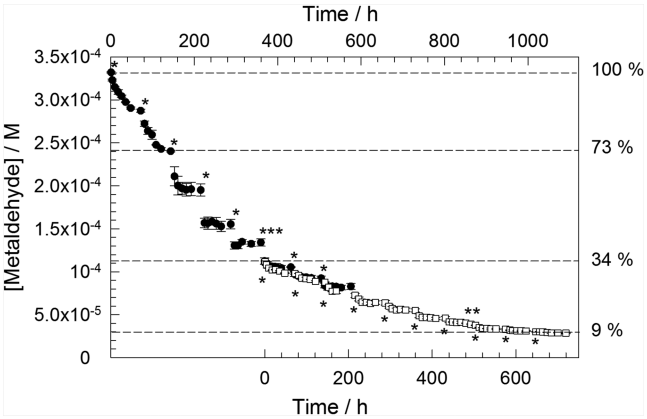

Figure 3. Kinetic traces of metaldehyde degradation by NaClO catalyzed by **1a** in pH 7.0 D_2O (0.01 M, phosphate). Two experiments are shown. Experiment 1: solid circles (●) and top time axis, $[Met]_0$ = 3.32×10^{-4} M, [**1a**] = 4.0×10^{-7} M, [NaClO] = 7.61×10^{-3} M. Experiment 2: hollow squares (□) and bottom time axis, $[Met]_0$ = 1.12×10^{-4} M, [**1a**] = 4.0×10^{-7} M, [NaClO] = 4.71×10^{-3} M. For both experiments: *indicates the addition of one 4.0×10^{-7} M catalyst dose, **indicates the addition of NaClO sufficient to raise the [NaClO] by 3.44×10^{-3} M, ***indicates the addition of one catalyst dose giving a [**1a**] of 4.0×10^{-7} M and NaClO sufficient to raise the [NaClO] by 4.79×10^{-3} M NaClO.

In Experiment 2, the oxidation of a fresh 1.12×10^{-4} M Met solution was studied (Figure 3 hollow squares and Figure S8) to examine if the accumulating acetate or inactivated catalyst products were contributing to the deterioration in Δ[Met] and TON.[41] For each catalyst dose of Experiment 2, the $[Met]_0$, Δ[Met], TON, and %Cvn are also summarized in Table S4. There is considerable agreement between the data sets. If the concentration of Met is followed along the black dotted curve of Experiment 1 through the white squares of Experiment 2, the result is representative of one continuous degradation process. Here, a ca. 1 order of magnitude reduction in [Met] (330−30 μM) by less than 0.02 M NaClO can be achieved in ∼47 days through treatment with 16 doses of **1a** each giving a solution [**1a**] of 4.0×10^{-7} M. The combined process would consume less than 60 equiv of NaClO and proceed with a TON of 66. This is significantly less than the Experiment 1 dose 1 TON of 112 ± 6. Both Δ[Met] and TON decline steadily with $[Met]_0$ (Table S4) for all Experiment 1 and 2 catalyst doses. The average k_i value of $(3 \pm 1) \times 10^{-4}$ M is identical to the single catalyst dose value calculated from the data in Table 1. The combined data set has the following broad implications for ultradilute TAML catalysis with $Fe_{Tot} < 1 \times 10^{-6}$ M (where no k_{2i} processes are observed).

First, dilution of the substrate poses a formidable challenge to ultradilute catalysis by diminishing the rate of substrate transformation without altering the rate of catalyst inactivation. By adapting eq 3, a relation previously derived for the determination of k_i values[32] and recently used to determine the k_i values for 15 TAML catalysts in the pH 7 oxidation of Orange II (OrII),[33] forms which model the change in substrate concentration (ΔS, eq 4), % conversion (%Cvn, eq 5) and the TON (eq 6) can be obtained and fit to the Met data where $S_0 = [Met]_0$, $S_\infty = [Met]_\infty$, and ΔS = ΔMet. These forms turn out to be very useful in better understanding the meaning of TON where the catalyst is degrading. In the oxidation of any substrate under any one set of conditions, both k_{II} and k_i are fixed. For a fixed catalyst dose (Fe_{Tot}), the ratio of these dictates the change in substrate concentration (Δ*S*) and the TON, both of which decline with the initial substrate concentration (S_0) as shown in eqs 4 and 6. The Met data confirm this (Figure 4). The mathematical treatment that resulted in eq 3 considered all of the events shown in Scheme 1 except the k_{2i} process to arrive at the most general expression.[32] Contributions from the catalyst activation process k_I are absent from this form indicating that S_∞, and thus ΔS and TON, are determined by the competition for Ac between the substrate oxidation ($-d[S]/dt = k_{II}[S][Ac]$) and catalyst inactivation ($d[Ic]/dt = k_i[Ac]$) processes alone. The rate of the former depends on the [S] while that of the latter does not. As a result, ΔS declines with S_0. This dynamic is especially important when the substrate is ultradilute as is the usual case with MPs in municipal wastewater.

$$\Delta S = S_0\left(1 - e^{-\frac{k_{II}}{k_i}Fe_{Tot}}\right) \quad (4)$$

DOI: 10.1021/jacs.6b11145
J. Am. Chem. Soc. 2017, 139, 879−887

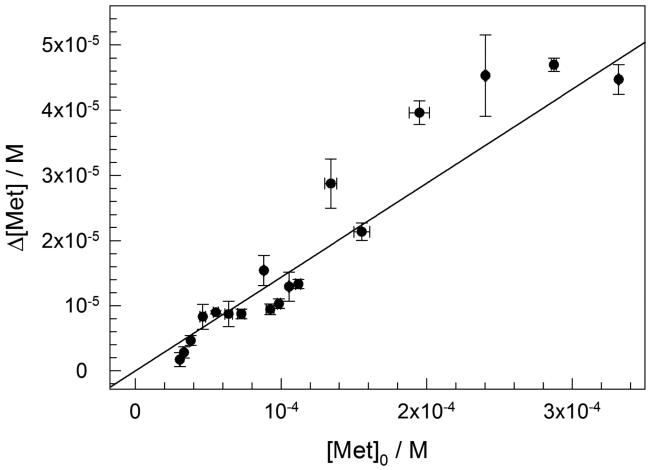

Figure 4. Correlation between the Δ[Met] and the $[Met]_0$. Each data point represents the Δ[Met] for each Experiment 1 or 2 catalyst dose. The line gives the eq 5 predicted Δ[Met] values with $k_i = 3.0 \times 10^{-4}$ s^{-1}, $k_{II} = 120$ M^{-1} s^{-1}, and [**1a**] = 4.0×10^{-7} M. The other conditions are as indicated in the Figure 3 caption and Table S4.

$$\%Cvn = \frac{\Delta S}{S_0} \times 100\% = (1 - e^{-\frac{k_{II}}{k_i}Fe_{Tot}}) \times 100\% \quad (5)$$

$$TON = \frac{(1 - e^{-\frac{k_{II}}{k_i}Fe_{Tot}})}{Fe_{Tot}} S_0 \quad (6)$$

Second, from pH 5.2−7, the oxidant independent ***1a*** *inactivation process operates via a mechanism that is sensitive to the Lewis acidity at Fe.* The linearity found in Figure 4 indicates that a constant k_{II}/k_i ratio holds for all of the catalyst doses of both experiments. The data were collected at varying pH, [NaClO], [product], and [Ic] such that the linear relationship of Figure 4 also establishes that these parameters do not alter k_{II}/k_i implying that inhibition by product or inactive catalyst species and NaClO dependent inactivation processes are negligible. The data in Figure 4 were collected at pH values over the range of 5.2−7. TAML k_{II} values have been observed to increase with pH by more than an order of magnitude from pH 6−7.[42] Therefore, the **1a**/NaClO k_{II} and k_i must track each other closely over this range as was found in catalysis by 15 TAML activators with H_2O_2 at pH 7.[33] We have interpreted these fixed k_{II}/k_i ratios as evidence that the Lewis acidity at Fe exerts a common influence over both k_{II} and k_i processes at pH 7, but for the H_2O_2 systems we were unable to determine whether the ratio mandated changes in k_i derive from the H_2O_2 dependent or independent processes, or both. Since contributions from NaClO dependent inactivation are negligible, the mandatory changes in k_i must originate from NaClO independent processes which operate from pH 5.2 to 7. Because the NaClO and H_2O_2 Ac are similar and the observed dependence on Lewis acidity is independent of oxidant, it is therefore likely that similar processes are operating in the H_2O_2 systems.

Third, while most MPs can be effectively treated by existing TAML systems operating under ultradilute aqueous conditions, those having k_{II}/k_i ratios ≤1 × 10^6 M^{-1} cannot. As noted, when [**1a**] > 1×10^{-6} M, contributions to k_i from decomposition processes that are second order in [**1a**] (k_{2i} processes) become significant. Therefore, we consider an Fe_{Tot} of 1×10^{-6} M to be an upper bound for effective ultradilute catalysis. In principle, below this, eqs 3−6 model the S_o/S_∞ ratio, %Cvn, and TON in TAML catalysis for the oxidation of any substrate by any oxidant with any catalyst under any conditions provided inactivation also occurs from Ac and neither the substrate nor the products perturb the catalytic cycle (e.g., substrate binding to the catalyst). However, it should be noted that the critical dimension of time is not captured by eqs 3−6 and thus cannot be included in the following discussion—we are further considering how to address the time dimension.

Using the known k_{II} and k_i values, eq 5 predicts within ±3% the observed experimental 5 %Cvn of Met found for **1a**/H_2O_2 treatment ([**1a**] = 4×10^{-7} M) in pH 7 buffered D_2O (0.01 M phosphate), the (14.4 ± 0.9) %Cvn of Met for **1a**/NaClO treatment ([**1a**] = 4×10^{-7} M) in pH 7 buffered D_2O (0.01 M phosphate), the 18 %Cvn of the persistent SSRI Sertraline (Ser) for **1a**/H_2O_2 treatment ([**1a**] = 3×10^{-7} M) in pH 7 buffered H_2O (0.01 M phosphate), the 27 %Cvn of the azo dye Orange II (OrII) for **1b**/H_2O_2 treatment ([**1b**] = 2×10^{-8} M) in pH 7 buffered H_2O (0.01 M phosphate), the >98 %Cvn of 17α-ethynylestradiol (EE2) for **1b**/H_2O_2 treatment ([**1b**] = 8×10^{-8} M) in pH 7 buffered H_2O (0.01 M phosphate),[43] and the 17 %Cvn of the dye Safranin O (SO) in pH 11 buffered H_2O ([**1a**] = 7.5×10^{-8} M).[36] Figure 5 is a helpful graphical representation of eq 5 onto which these processes can be plotted. The k_{II} value for **1a** oxidation Met in both the H_2O_2 and NaClO systems, 120 M^{-1} s^{-1}, is the lowest of any MP we have ever tested. The k_{II} value for **1b**/H_2O_2 oxidation of EE2 at

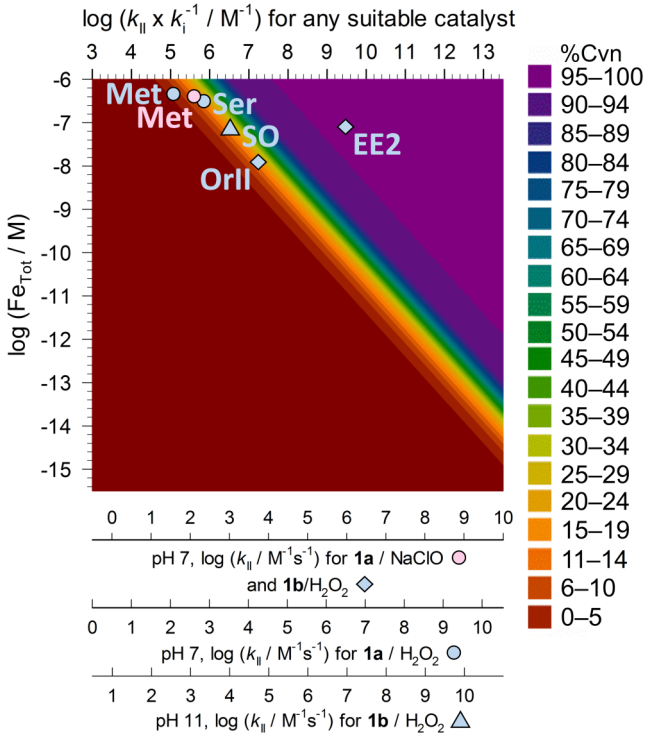

Figure 5. The eq 5 predicted %Cvn as a function of $\log(Fe^{III}_{Tot})$ and either $\log(k_{II}/k_i)$ for treatment with any suitable catalyst (top axis), $\log(k_{II})$ for pH 7 treatment with **1a**/NaClO, $\log(k_{II})$ for pH 7 treatment with **1b**/H_2O_2, $\log(k_{II})$ for pH 7 treatment with **1a**/H_2O_2, or $\log(k_{II})$ for pH 11 treatment with **1b**/H_2O_2 (bottom axes which shift with different oxidants and pH's). The points shown indicate experimental data for conversion of various substrates having the identities indicated in the text. The k_{II}, k_i, and %Cvn values for each data point were obtained individually.

DOI: 10.1021/jacs.6b11145
J. Am. Chem. Soc. 2017, 139, 879−887

pH 7, 8.6 × 10^5 M^{-1} s^{-1}, is the highest.[12] The value for **1a**/H_2O_2 oxidation of Ser, 740 M^{-1} s^{-1}, is closer to the Met than the EE2 value as expected. The value for **1b**/H_2O_2 oxidation of OrII, 4,950 M^{-1} s^{-1}, is closer to the EE2 than the Met value as expected. Thus, eqs 3-6 hold over a ca. 10^4 M^{-1} range of k_{II}/k_i for two catalysts and oxidants and at pH 7 and 11, adding confidence to both the validity and generality of the analytical model for both academic and real-world applications.

Typically, water treatment plants are driven by a need to achieve regulated levels rather than complete removal of ultradilute pollutants. Equation 5 could be used to predict the optimal catalyst loading, Fe_{Tot} (below 1 × 10^{-6} M), needed to effect a given %Cvn of any MP under any one set of conditions from data obtained by measuring one incomplete kinetic trace at a known Fe_{Tot} which gives k_{II}/k_i. This will always hold provided the process is rapid enough to be deployable. If k_i is known under these conditions, k_{II} is also known—an extensive series of pH 7 k_i values for TAMLs have been determined.[33] We are treating a larger set of MPs and examining the behavior of additional catalysts over a wider pH range to obtain k_{II}, k_i, and %Cvn under different conditions to further cement the usefulness of this predictive tool.

The upper bound of the log(k_{II}/k_i) range shown in Figure 5 (top horizontal axis) is set at the hypothetical diffusion controlled limit for **1a**/NaClO treatment at pH 7 (k_{II} of ca. 10^{10} M^{-1} s^{-1}, topmost axis below figure).[44] In applying TAML processes to remove micropollutants, useful processes deliver % Cvn ≥50. The equation predicts that subpicomolar [**1a**] can effect 50 %Cvn for very rapidly oxidizing substrates. However, practical concerns such as reaction time will likely limit utility here—we are working to discover a similar tool for reaction time. The lower k_{II}/k_i limit of the green band (50 %Cvn) is found at ca. 10^6 M^{-1}. The k_{II}/k_i ratios for TAML catalyzed oxidation of many MPs lie above this. However, this sets the lower k_{II} bound for the most useful **1a**/H_2O_2 treatment with an Fe_{Tot} of 1 × 10^{-6} M at ca. 1100 M^{-1} s^{-1} near pH 7. Substrates more slowly oxidized than this are not well treated with a single catalyst dose of **1a**/H_2O_2. The lower k_i of **1a**/NaClO treatment shifts this bound to ca. 300 M^{-1} s^{-1}. However, Met remains just out of reach with a k_{II} of 120 ± 30 M^{-1} s^{-1}. As the **1a**/NaClO data demonstrate, the key to extending ultradilute catalysis to more slowly transformed substrates is the development of systems that maximize the k_{II}/k_i ratio by disproportionately increasing k_{II}, decreasing k_i, or both. An effective Met solution would require roughly a doubling of the **1a** k_{II} value or halving of the **1a**/NaClO k_i value while keeping the other constant. We are working toward achieving and exceeding this entirely realistic goal via iterative catalyst design.

Fourth, when Fe_{Tot} ≤ ca. 1 × 10^{-6} M, successive small catalyst doses are not more effective than larger catalyst doses. As indicated by eq 6 and Figure 6, the dependence of TON on the k_{II}/k_i ratio and Fe_{Tot} is complex. We have interpreted the relationship in the following way. For any one catalyst operating under any one set of conditions, k_i is fixed. The value of the k_{II}/k_i ratio then varies with k_{II}. Thus, the value of k_{II} determines the dependence between TON and Fe_{Tot} and places the oxidation process on a spectrum between two limits. At the low k_{II} limit, when $k_{II}Fe_{Tot}/k_i < 1$, eq 6 can be approximated by the first term of a Maclaurin series, TON ≈ $k_{II}S_0/k_i$ (contributions from the higher order terms of the series are negligible). Consequently, in the **1a**/NaClO conversion of slowly transformed Met, for which k_{II}/k_i = 4 × 10^5 M^{-1}, the TON is largely independent of Fe_{Tot} as shown in Table 2 and along the surface of Figure 6 at the low k_{II}/k_i limit. In these oxidations, every catalyst molecule of any catalyst dose does about the same amount of work, and the %Cvn scales linearly with Fe_{Tot}.

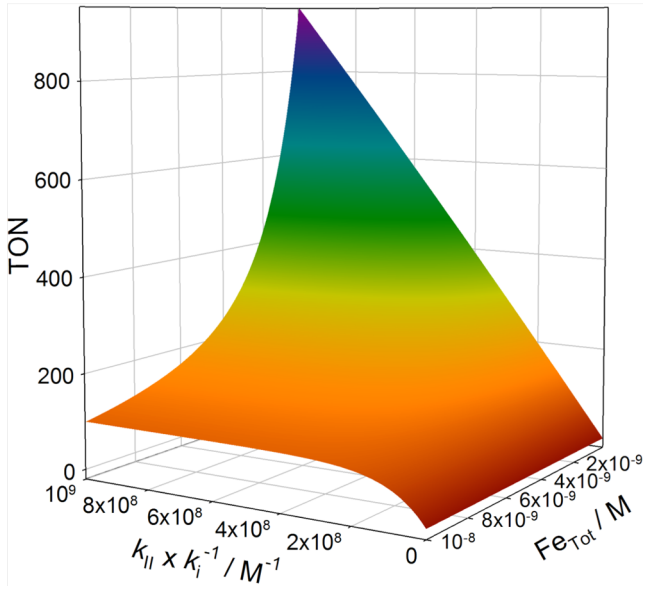

Figure 6. Equation 6 calculated dependence of the TON on k_{II}/k_i and Fe_{Tot} for a fixed S_0 of 1 × 10^{-6} M. From [Fe_{Tot}] 10^{-8}–10^{-6} M (not shown), the surface shape changes little from that shown at [Fe_{Tot}] = 10^{-8} M.

At the high k_{II} limit where $e^{-(k_{II}/k_i)Fe_{Tot}} \leq 0.1$, the numerator of eq 6 approaches 1 and TON ≈ S_0/Fe_{Tot}. For example, for the **1b**/H_2O_2 treatment of EE2 introduced above, k_{II}/k_i = 2.9 × 10^9 M^{-1} and $e^{-(k_{II}/k_i)Fe_{Tot}}$ = 2.5 × 10^{-100}. For treatment of such rapidly oxidized substrates, as Fe_{Tot} increases, so does ΔS and with it the dilution of the substrate during functioning catalysis. This decreases the rate of substrate oxidation relative to that of catalyst inactivation causing average TONs to drop. This could lead one to suspect that treatment with multiple small catalyst doses would lead to improved performance. However, the use of multiple small catalyst doses is not more efficient at achieving a set %Cvn than adding the equivalent Fe_{tot} in a single dose provided the sum of all doses is less than ca. 1 × 10^{-6} M because dilution lowers the average TON regardless of how the catalyst is administered (see the SI for a mathematical explanation of this). When eq 3 holds, a single TAML catalyst dose is optimal for most rapidly achieving a desired %Cvn.

■ CONCLUSION

This study explores the behavior of TAML catalysis at the performance boundary prescribed by the exceptionally recalcitrant pollutant, Met. The findings communicated herein have broad significance for TAML catalysis. The rates of **1a** catalyzed Met transformation by NaClO and H_2O_2 are identical giving a strong indication that the same reactive intermediate attacks Met in both systems. However, TAML/NaClO delivers a 3-fold k_{II}/k_i enhancement by lowering the rate of catalyst inactivation, which we attribute to elimination of contributions from H_2O_2 dependent inactivation processes. At [**1a**] > 1 × 10^{-6} M, inactivation pathways that are bimolecular in catalyst (k_{2i}) and outpace those unimolecular in catalyst (k_i) render **1a**/H_2O_2 transformation of Met completely ineffective; this establishes an upper bound for [TAML] in H_2O_2 systems of 1 μM. The use of NaClO enhances the technical performance

DOI: 10.1021/jacs.6b11145
J. Am. Chem. Soc. 2017, 139, 879–887

of processes with [**1a**] > 1 μM by restoring functioning catalysis indicating that both k_i and k_{2i} are lower in the NaClO system. In both the H_2O_2 and NaClO systems, k_{2i} processes outpace k_i processes. Further investigations of the mechanisms of the k_{2i} processes and their dependences on the identity of the oxidant are underway. Application of eq 3 and forms derived from it to the Met data indicates that while ΔS decreases with S_0, %Cvn remains constant. The expression for TON provides a more detailed understanding of chemical processes which underlie as well as the impact of substrate dilution on this venerable metric for evaluating catalyst performance. This work demonstrates the advances in understanding which can be achieved through detailed analysis of the mechanisms of both catalyst operation and inactivation; the latter is a critical and underexplored territory.

■ ASSOCIATED CONTENT

Supporting Information

The Supporting Information is available free of charge on the ACS Publications website at DOI: 10.1021/jacs.6b11145.

Details of metaldehyde degradation (Figures S1−S8); metaldehyde degradation summary (Tables S1−S4) (PDF)

■ AUTHOR INFORMATION

Corresponding Author

*tc1u@andrew.cmu.edu

ORCID

Matthew R. Mills: 0000-0001-8975-2855

Notes

The authors declare no competing financial interest.

■ ACKNOWLEDGMENTS

T.J.C. thanks the Heinz Endowments for support. M.R.M thanks the Steinbrenner Institute and the R. K. Mellon Foundation for Doctoral Fellowships. NMR instrumentation at CMU was partially supported by the NSF (CHE-0130903 and CHE-1039870).

■ REFERENCES

(1) Snyder, S. A.; Wert, E. C.; Lei, H.; Westerhoff, P.; Yoon, Y. *Removal of EDCs and Pharmaceuticals in Drinking and Reuse Treatment Processes*, 1st ed.; AwwaRF: Denver, 2007.

(2) Schwarzenbach, R. P.; Escher, B. I.; Fenner, K.; Hofstetter, T. B.; Johnson, C. A.; von Gunten, U.; Wehrli, B. *Science* **2006**, *313*, 1072−1077.

(3) McArdell, C. S. *Norman Bulletin* **2015**, 36−37.

(4) Kundu, S.; Chanda, A.; Thompson, J. V. K.; Diabes, G.; Khetan, S. K.; Ryabov, A. D.; Collins, T. J. *Catal. Sci. Technol.* **2015**, *5*, 1775−1782.

(5) Kundu, S.; Chanda, A.; Khetan, S. K.; Ryabov, A. D.; Collins, T. J. *Environ. Sci. Technol.* **2013**, *47*, 5319−5326.

(6) Kundu, S.; Chanda, A.; Espinosa-Marvan, L.; Khetan, S. K.; Collins, T. J. *Catal. Sci. Technol.* **2012**, *2*, 1165−1172.

(7) Shen, L. Q.; Beach, E. S.; Xiang, Y.; Tshudy, D. J.; Khanina, N.; Horwitz, C. P.; Bier, M. E.; Collins, T. J. *Environ. Sci. Technol.* **2011**, *45*, 7882−7887.

(8) Beach, E. S.; Malecky, R. T.; Gil, R. R.; Horwitz, C. P.; Collins, T. J. *Catal. Sci. Technol.* **2011**, *1*, 437−443.

(9) Beach, E. S.; Duran, J. L.; Horwitz, C. P.; Collins, T. J. *Ind. Eng. Chem. Res.* **2009**, *48*, 7072−7076.

(10) Chanda, A.; Khetan, S. K.; Banerjee, D.; Ghosh, A.; Collins, T. J. *J. Am. Chem. Soc.* **2006**, *128*, 12058−12059.

(11) Banerjee, D.; Markley, A. L.; Yano, T.; Ghosh, A.; Berget, P. B.; Minkley, E. G.; Khetan, S. K.; Collins, T. J. *Angew. Chem., Int. Ed.* **2006**, *45*, 3974−3977.

(12) Mills, M. R.; Arias-Salazar, K.; Baynes, A.; Shen, L. Q.; Churchley, J.; Beresford, N.; Gayathri, C.; Gil, R. R.; Kanda, R.; Jobling, S.; Collins, T. J. *Sci. Rep.* **2015**, *5*, 10511.

(13) Churchley, J.; Collins, T. J.; Jobling, S. *Catalytic Oxidation of Pharmaceutical Compounds in Wastewater Effluents*; London, UK, 2011.

(14) Tang, L. L.; DeNardo, M. A.; Gayathri, C.; Gil, R. R.; Kanda, R.; Collins, T. J. *Environ. Sci. Technol.* **2016**, *50*, 5261−5268.

(15) Autin, O.; Hart, J.; Jarvis, P.; MacAdam, J.; Parsons, S. A.; Jefferson, B. *Appl. Catal., B* **2013**, *138-139*, 268−275.

(16) James, C. P.; Germain, E.; Judd, S. *Sep. Purif. Technol.* **2014**, *127*, 77−83.

(17) Scheideler, J.; Bosmith, A. *Aqua Gas* **2014**, *94*, 52−57.

(18) Collins, T. J.; Gordon-Wylie, S. W.; Horwitz, C. P. U.S. Patent 6054580, 2000.

(19) Deborde, M.; von Gunten, U. *Water Res.* **2008**, *42*, 13−51.

(20) Collins, T. J.; Gordon-Wylie, S. W. U.S. Patent 5,847,120, 1998.

(21) Mills, M. R.; Burton, A. E.; Mori, D. I.; Ryabov, A. D.; Collins, T. J. *J. Coord. Chem.* **2015**, *68*, 3046−3057.

(22) Ghosh, M.; Singh, K. K.; Panda, C.; Weitz, A.; Hendrich, M. P.; Collins, T. J.; Dhar, B. B.; Sen Gupta, S. *J. Am. Chem. Soc.* **2014**, *136*, 9524−9527.

(23) Kundu, S.; Annavajhala, M.; Kurnikov, I. V.; Ryabov, A. D.; Collins, T. J. *Chem. - Eur. J.* **2012**, *18*, 10244−10249.

(24) Fukuta, N. *Nature* **1963**, *199*, 475−476.

(25) Craven, E. C.; Jowitt, H.; Ward, W. R. *J. Appl. Chem.* **1962**, *12*, 526−535.

(26) Pauling, L.; Carpenter, D. C. *J. Am. Chem. Soc.* **1936**, *58*, 1274−1278.

(27) George, P. *Biochem. J.* **1953**, *55*, 220−230.

(28) Kelm, M.; Pashalidis, I.; Kim, J. I. *Appl. Radiat. Isot.* **1999**, *51*, 637−642.

(29) Arnett, E. M.; Barkley, W. E.; Beak, P.; Becker, E. D.; Bryndza, H. E.; Chang, I. L.; Creutz, C.; Danheiser, R. L.; Gordon, E. M.; Lackmeyer, R. J.; Magid, Lee; McBride, T. F.; Norberg, A. M.; Petrillo, E. W.; Pine, S. H.; Thompson, F. M.; Wong, T. M.; Gowen, K.; Plimpton, S. W.; Butera, J. F. *Prudent Practices in the Laboratory: Handling and Disposal of Chemicals*; National Academy Press: Washington, D.C., 1995.

(30) Sedlak, D. L.; von Gunten, U. *Science* **2011**, *331*, 42−43.

(31) Yang, X.; Shang, C. *Environ. Sci. Technol.* **2004**, *38*, 4995−5001.

(32) Emelianenko, M.; Torrejon, D.; DeNardo, M.; Socolofsky, A.; Ryabov, A.; Collins, T. *J. Math. Chem.* **2014**, *52*, 1460−1476.

(33) DeNardo, M. A.; Mills, M. R.; Ryabov, A. D.; Collins, T. J. *J. Am. Chem. Soc.* **2016**, *138*, 2933−2936.

(34) Abe, K.; Hagiwara, J.; Machida, W. *Taiki Osen Gakkaishi* **1980**, *15*, 21−4.

(35) Bartos, M. J.; Gordon-Wylie, S. W.; Fox, B. G.; Wright, L. J.; Weintraub, S. T.; Kauffmann, K. E.; Munck, E.; Kostka, K. L.; Uffelman, E. S.; Rickard, C. E. F.; Noon, K. R.; Collins, T. J. *Coord. Chem. Rev.* **1998**, *174*, 361−390.

(36) Chanda, A.; Ryabov, A. D.; Mondal, S.; Alexandrova, L.; Ghosh, A.; Hangun-Balkir, Y.; Horwitz, C. P.; Collins, T. J. *Chem. - Eur. J.* **2006**, *12*, 9336−9345.

(37) Horwitz, C. P.; Fooksman, D. R.; Vuocolo, L. D.; Gordon-Wylie, S. W.; Cox, N. J.; Collins, T. J. *J. Am. Chem. Soc.* **1998**, *120*, 4867−4868.

(38) Gupta, S.; Stadler, M.; Noser, C. A.; Ghosh, A.; Steinhoff, B.; Lenoir, D.; Horwitz, C. P.; Schramm, K. W.; Collins, T. J. *Science* **2002**, *296*, 326−328.

(39) Miller, J. A.; Alexander, L.; Mori, D. I.; Ryabov, A. D.; Collins, T. J. *New J. Chem.* **2013**, *37*, 3488−3495.

(40) Tynkkynen, T.; Tiainen, M.; Soininen, P.; Laatikainen, R. *Anal. Chim. Acta* **2009**, *648*, 105−12.

(41) Crabtree, R. H. *Chem. Rev.* **2015**, *115*, 127−150.

(42) Warner, G. R.; Mills, M. R.; Enslin, C.; Pattanayak, S.; Panda, C.; Panda, T. K.; Gupta, S.; Ryabov, A. D.; Collins, T. J. *Chem. - Eur. J.* **2015**, *21*, 6226−6233.
(43) Mills, M. R. Synthesis, Characterization, and Unique Properties of a Novel, Completely Aliphatic TAML Activator and Applications of TAML Catalysis for Oxygen Evolution and Pollution Remediation. Carnegie Mellon University, Pittsburgh, PA, 2016.
(44) Koenig, S. H.; Brown, R. D. *Proc. Natl. Acad. Sci. U. S. A.* **1972**, *69*, 2422−2425.

DOI: 10.1021/jacs.6b11145
J. Am. Chem. Soc. 2017, 139, 879−887